

MULTI-TAPER COHERENCE RECEIVER FUNCTIONS AND P-WAVE SCATTERING WITHIN THE CRUST

Jeffrey Park, Vadim Levin, Joydeep Bhattacharyya,
Department of Geology and Geophysics, Yale University

Sponsored by U. S. Department of Defense
Defense Threat Reduction Agency
Contract No. DSWA01-98-011

ABSTRACT

Teleseismic P-waves are followed by a series of scattered waves, particularly P-to-S converted phases, that form a coda. The sequence of scattered waves on the horizontal components is represented by the receiver function (RF) for the station, and may vary with the approach angle and azimuth of the incoming P wave. This coda can be generated via side-scattering from topographic features. However, at teleseismic frequencies (<2 Hz) many, if not most, converted phases in the first few seconds after P are generated via forward scattering from seismic interfaces within the crust and uppermost mantle, where density and elastic properties undergo discontinuity. P-coda on the transverse horizontal component indicates either the presence of dipping interfaces, the presence of anisotropy, or 3-D structures. The three different cases can be distinguished, given sufficient data, by the move-out of scattered waves with back-azimuth and incoming phase velocity. Comparing RFs for different records can be misleading if the frequency content of different P waves varies greatly. Popular methods for RF-generation include deconvolution and spectral division, with damping to avoid numerical instabilities. Deconvolution operators are often biased towards the frequencies where signal is strongest, similar to spectral-division schemes with constant water-level damping. Worse, estimates of uncertainty are scarce, which impedes developing a weighted average of RF-estimates from multiple events.

We have developed a frequency-domain RF inversion algorithm using multi-taper coherence estimates instead of spectral division, using the pre-event noise spectrum for frequency-dependent water-level damping. The multi-taper spectrum estimates are leakage resistant, so low-amplitude portions of the P-wave spectrum can contribute usefully to the RF estimate. The coherence between vertical and horizontal components can be used to obtain a frequency-dependent uncertainty for the RF. Tests of this technique using teleseismic data from PET (Petropavlovsk-Kamchatsky, Russia) show excellent RF retrieval for signals up to $f=2.0$ Hz. Several crustal P-SH conversions can be seen in the transverse RF, as well as a “derivative pulse” signal with extreme move-out that we interpret as a wave scattered at the top of the Kamchatka slab. The “derivative pulse” character of this and other signals in the transverse RF suggests interfering P-S conversions at closely spaced interfaces. We will report RF sweeps from PET and other permanent broadband stations.

Key Words: P waves, receiver function

UR-99-384 or UCRL-ID-132897.

location, source mechanism, waveform inversion, depth phases, phase detection

OBJECTIVE

Proper detection and discrimination of seismic waves from suspected clandestine explosions is best accomplished when the wave-propagation characteristics of the Earth between the source and the seismometer are well-known. Teleseismic body waves from earthquakes and explosive sources experience scattering as they travel upwards through the uppermost mantle and crust. Similarly, regional body waves experience scattering as they travel through the crustal waveguide. The objective of this research project is to use variations in the elastic anisotropy of the crust and uppermost mantle to describe the scattering that is observed in seismic data. Most models for seismic scattering invoke a statistical 3-D distribution of small-scale anomalies in isotropic P and S seismic velocities e.g., the phase-screen approach (Wu, 1994) or finite-difference computations (e.g. Levander and Hollinger, 1992). The motivation for using anisotropy is threefold. First, fairly modest fluctuations in anisotropic properties can cause significant conversion of P (compressional) motion to S (shear) motion in propagating seismic waves. Second, numerical experiments have shown that flat-layered anisotropic media can cause large scattered wavetrains in both surface waves (Park, 1996) and body waves (Levin and Park, 1997a; 1998). Third, elastic anisotropy, as a material property of rocks, seems to be the rule rather than the exception, caused by aligned cracks (Hudson, 1981), by lattice-preferred mineral orientation within rocks (Babuska and Cara, 1991), and by fine-layering (Helbig, 1994). Large-scale 3-D velocity structures are not necessary to create a P-coda or an extended surface-wave signal, at least in theory. If a 1-D anisotropic seismic-velocity structure can usefully represent much of the scattered seismic energy in an incoming signal at a particular seismic observatory, there are practical benefits. An analyst, faced with a complex seismic signal to interpret, would likely need to know fewer parameters of earth structure local to the station, and may run simpler synthetic seismogram codes to reproduce the data.

A key objective of this research is to determine whether layered anisotropy is pervasive in the crust and has a strong influence on body-wave coda. To do this, we estimate the scattering of teleseismic P waves as they travel upwards through the crust, using a modification of familiar receiver-function techniques (Langston, 1977; Ammon, 1991; Abers, et al 1995). Computational modeling (Cassidy, 1992; Kosarev et al 1994; Levin and Park, 1997a; 1998; Savage, 1998) demonstrates that both anisotropy and dipping interfaces cause predictable variations in P-to-S scattered energy, dependent on the incoming direction of the P-wave -- its angle of incidence (or equivalently, its "slowness" p), and its back-azimuth angle ϕ . The P-to-SH energy scattered to the transverse-horizontal component of motion is particularly diagnostic, as its amplitude is predicted to reverse from positive to negative, and vice versa, in a lobate pattern with back-azimuth ϕ . We therefore analysed seismic data from representative permanent seismic observatories to study the back-azimuth dependence of receiver functions. A dipping interface and a 3-D scatterer can be distinguished from flat-layered anisotropy by examining the "moveout" of the scattered wave. The radial- and transverse-horizontal scattered waves arrive later for waves that approach updip a slanted interface, relative to waves that approach downdip. The timing of a wave generated by an isolated 3-D scatterer also depends strongly on the back-azimuth of the incoming P wave. By contrast, a P-to-S scattered wave experiences very little moveout, if any, from a horizontal interface between layers of anisotropic rock. If receiver functions from a particular seismic observatory exhibit a lobate amplitude pattern in the transverse component, and there is negligible moveout with back-azimuth in the delay time, a flat-layered anisotropic crust gains respect as a good model to represent scattering at that location.

Although this research focusses on developing anisotropic models for crustal seismic velocities, the receiver functions themselves may be useful in the verification and monitoring activities associated with a Comprehensive Nuclear-Test-Ban Treaty (CTBT). Receiver functions represent empirically the scattering at particular seismic stations. They are useful to the extent that they are reproducible in many seismic records, even if no simple earth-structure model can explain them.

RESEARCH ACCOMPLISHED

Early in the fiscal year we studied P-to-S scattered waves in seismograms recorded at the Southern California Seismic Network (SCSN) station JRC, a broadband seismic observatory sited within the Coso

geothermal field. We constructed an anisotropic crustal model to fit this data using the genetic-algorithm tools developed by Levin and Park (1997a). In this model we find a low-velocity zone in the mid-crust, presumably related to the heat source of the geothermal activity. P-SH scattering effects in the RFs can be modeled with a 15-km anisotropic (2%) mid-crustal layer and a highly anisotropic (6%) thin surface layer that has fast axes (N60°W) aligned near the NE-SW direction of shear in regional seismicity.

Later in the first year of our project we improved our algorithm for determining the receiver functions (RFs) that describe P-to-S scattering by the shallow layers of the Earth, with particular emphasis on P-to-SH scattering that appears on the transverse horizontal component. Receiver functions are easy to define, but much more difficult to compute in a reliable, robust manner. The receiver function describes the tendency of an upward-travelling P-wave to set off a chain of subsidiary waves, mostly S waves, that arrive after the main P wave. Favored methods to compute receiver functions use the record of vertical vibration on the seismogram, which contains mostly P-wave motion, to predict the records of radial- and transverse-horizontal seismic motion. The simplest way to accomplish this is by spectral division: form a ratio of the Fourier transforms of the different components: $H_R(f) = R(f)/Z(f)$ and $H_T(f) = T(f)/Z(f)$. Here $Z(f)$, $R(f)$, and $T(f)$ are the Fourier spectra of the vertical, radial and transverse seismic components, respectively. The spectral-domain receiver functions $H_R(f)$ and $H_T(f)$ can be transformed into a “prediction filter” of P-to-S scattered waves by performing the inverse Fourier transform on them.

Although simple to apply, spectral division is a bad method. It is numerically unstable near the zeroes of $Z(f)$. It also fails to account for seismic noise. To circumvent this, a modified spectral division is preferred, using a “water level” to avoid the zeroes of $Z(f)$ (e.g. Ammon, 1991). Alternatively, one can deconvolve the horizontal seismic records from the vertical record in the time domain (e.g. Abers et al 1995) to compute the scattering “prediction filter” directly. Each of these techniques has shortcomings, as each tends to be bandlimited. The “water level” in spectral division obscures low-amplitude spectral components. Similarly, time-domain deconvolution tends to be dominated by the Fourier components with largest amplitude. In practice this has limited many RF-studies to use data low-passed at $f \sim 0.5$ Hz. This has led to some spectacular images of upper-mantle discontinuities at 420 and 670-km depth (e.g., Dueker and Sheehan, 1997), but is problematic for probing fine-layered crustal structure.

We developed a technique that appears to overcome the problems of typical RF estimation. The technique is a spectral-domain method, using the complex-valued multiple-taper spectral cross-correlation, rather than spectral division, as a more robust estimator of the causal relation between the horizontal and vertical seismograms. We use a frequency dependent water-level to damp the inversion, using the spectrum of the pre-event noise as a scaling factor. We use multiple-taper spectral estimation (Thomson, 1982; Park et al, 1987; Vernon et al, 1991) to ensure that the estimates of water-level and coherence are minimally contaminated by spectral leakage. This allows us to estimate spectral ratios at frequencies where the signal is low, but the signal-to-noise ratio is still high. Estimating $H_R(f)$ and $H_T(f)$ using coherence has an additional advantage. At frequencies where the coherence between vertical and horizontal seismic components is low, one can presume that either background noise or signal-generated noise has obscured their relationship. In the RF-estimation examples we show below, the vertical-radial-transverse coherences vary up and down with frequency, in a manner largely unpredictable from visual perusal of the data. We developed a frequency-dependent uncertainty estimate for the receiver functions $H_R(f)$ and $H_T(f)$ that varies inversely with coherence $C(f)$. The uncertainty is small when $C(f)$ near unity, and large for smaller $C(f)$. The formal uncertainty estimate offers a way to form composite RFs from different seismic records in a weighted linear combination. We use the inverse-variances of the individual RFs as weights, so that poorly constrained estimates influence the weighted sum less than do $H(f)$ with smaller uncertainty.

We compute time-domain receiver functions by inverting the Fourier-domain RFs $H_R(f)$ and $H_T(f)$. To avoid ringing in the RF, we taper the spectrum up to a user-specified cutoff frequency with a cosine-squared function. For example, RFs with a frequency cutoff of 2 Hz include significant information only up to ~ 1.3 Hz, with half-amplitude at 1 Hz. In the frequency domain, error bars indicate the uncertainty of the RFs. In the time domain there are no formal error bars, but fluctuations in the RF at negative times offer a visual assessment of uncertainty in the wiggles that follow. When frequency-domain RFs from multiple

data records are combined in a weighted average, this spurious precursory portion of the prediction filter tends to decrease in the composite time-domain RF.

The advantages of our new RF-estimation technique can be assessed with examples from seismic data. Figure 1 shows P waves from two earthquakes recorded at station PET (Petropavlovsk-Kamchatsky, Russia) of the Global Seismographic Network (GSN). Neither P wavetrain is an ideal candidate for receiver-function estimation. Both P-waves are extended in time, rather than impulsive, and the 10/5/93 record has a low signal-to-noise ratio in the unfiltered time domain. The signal and pre-event spectra are compared in Figure 2, and show that the signal-to-noise ratio is high at frequencies $f > 1$ Hz, even though the P-waves are both dominated by frequencies $f < 0.7$ Hz. The coherences are variable, but often near unity even where the spectrum has low amplitude. The water-level damping technique would erase this information. Figure 3 demonstrates that the radial RFs for these two P-waves are reassuringly similar. For the 9/6/93 record, a sequence of 3-4 pulses spaced at ~ 2 -sec intervals is reconstructed from a signal that is dominated by energy at significantly longer period. The transverse RFs agree less well, but this is reflected in the spectral-domain error bars in Figure 3. The peak in $H_T(f)$ at 0.3 Hz coincides with the microseism peak at PET, and so is not retrieved well for the 10/5/93 record.

We have estimated distance- and back-azimuth dependent receiver functions for the permanent broadband seismological stations PET, RAYN (Ar Rayn, Saudi Arabia) and ARU (Arti Settlement, Russia). PET lies above the active, steeply dipping (55°) Kamchatka subduction zone (Gorbatov et al, 1997). RAYN lies within stable continental shield. ARU lies above an ancient (Paleozoic) continental suture zone, marked by the north-south trending Ural Mountains.

We had identified a strongly anisotropic lower-crustal layer beneath ARU in a previous study (Levin and Park, 1997b). Using the new RF-estimation technique, we were able to utilize 1989-98 data from 442 seismic events with $M=6.3$ or greater, including 112 core-refracted high-frequency PKP and PKiKP phases from events more distant than 95 degrees from ARU. Frequency-domain RFs from individual records are bin-averaged in overlapping 10° intervals of either epicentral distance or back-azimuth. The bins are spaced at 5° intervals. When the radial-component composite RF for ARU is plotted against epicentral distance (Figure 4), the moveout of the P-to-S converted wave at the Moho (~ 4 -5-sec time delay) is clearly evident. The delay is greater for closer events, because the P-wave incidence angle is more shallow, and the converted wave must travel a longer path from the base of the crust to the seismometer. One can also observe a distance-dependent modulation in the amplitude of the radial RF $H_R(t)$ at $t=0$. The largest $H_R(0)$ is found for closer events, in which the incoming P-wave has shallow incidence and a substantial radial projection. The minimum radial RF amplitude occurs at epicentral distances beyond 100° , where PKP waves are steeply incident. The back-azimuth sections for radial and transverse composite RFs (Figure 5) confirm the anisotropic crustal model of Levin and Park (1997b): a strong negative pulse on the radial RF at 2-sec delay indicates a mid-crustal seismic low-velocity zone of some kind, and is a strong derivative-pulse on the transverse RF that suffers an amplitude polarity reversal with back-azimuth. Levin and Park (1997b) modeled this feature with a strongly anisotropic lower crustal layer with seismic velocity suggestive of a steeply-tilted fine-layered mixture of crust and mantle rocks.

Although only two years of data are available for RAYN, an estimate of crustal reverberation structure can be made at this low-noise station from 65 events (not shown), even though only PKP waves are available at most back-azimuths. A clear polarity reversal in the transverse RF for pulses at 5- and 8-sec delay is seen. This suggests an interface between anisotropic layers and not a simple dipping interface, because there is no accompanying radial-RF pulse at 8-second delay. It is possible that the transverse signals are actually reverberations of some kind, but the lack of similar set of pulses in the radial RF argues against a simple reverberation.

We computed receiver functions from 241 data traces recorded at station PET, but data is sparse and/or poor in several sectors of back-azimuth e.g. 275° - 360° . Nevertheless, abundant earthquakes illuminate PET from the east, south and southwest. For back-azimuths between 150° and 200° , a strong transverse-component scattered wave moves out from 7-sec delay to 10-sec delay (Figure 7). This delay suggests an interface

much deeper than the Moho, and that the interface is strongly tilted. We identify it with the top of the Pacific plate as it subducts (as a “slab”) into the mantle along the east coast of Kamchatka. At shorter delay times (1-3 sec), the transverse RF flips polarity at roughly 200° back-azimuth, that is, for P waves that arrive roughly parallel to the strike of the dipping slab. Dipping geologic interfaces that are aligned with the downgoing slab are not good candidates to explain this behavior. The transverse RF polarity reversal might be better explained by a shallow interface that dips with strike perpendicular to the Kamchatka trench. Alternatively, a strongly anisotropic surface layer with a symmetry axis sub-parallel to the trench could cause the polarity switch.

Analysis for stations ARU, RAYN and PET demonstrates that the radial and transverse RFs do not often correlate peak to peak, as would be expected from a set of solitary waves deflected from a collection of isolated interfaces or obstacles. Instead, the transverse- and radial-component scattered waves are often shifted in phase by 90°, so that one resembles the derivative of the other. The slab-converted phase at PET has a “derivative pulse” shape on the transverse RF, and is as large as on the radial RF. This implies the phase is generated by interference between multiple scattered waves e.g. conversions at the top and bottom of a thin oceanic crust at the top of the subducting slab. Within the crust, the phase lag between radial and transverse RFs persists as the cutoff frequency increases to $f=3.0$ Hz and beyond. This suggests that the pulses are caused by the interference of numerous P-to-S converted phases caused by fine-scale layering of anisotropic rock units.

CONCLUSIONS AND RECOMMENDATIONS

Seismic stations ARU and RAYN appear both to lie atop a horizontally layered structure that nevertheless generates strong P-SH scattered energy on the transverse component. A 1-D anisotropic model of seismic velocity may therefore adequately describe wave-propagation effects near these stations. For station PET the situation is more complicated. RF estimates show clear evidence of the steeply-dipping subducting slab in the mantle. Tilted interfaces in the upper crust are suggested by perusal of Figure 8, especially at the 3.0-Hz cutoff, where the midcrustal 3.5-sec-delay conversion appears to arrive early for nearby earthquakes, but later for distant earthquakes, in a trend opposite to that of the Moho P-to-S conversion. This suggests a weakly-dipping mid-crustal interface. More analysis is needed to determine the total departure of this region from a horizontally-layered earth model, but significant 3-D structure appears necessary to model the crustal reverberations at PET in detail.

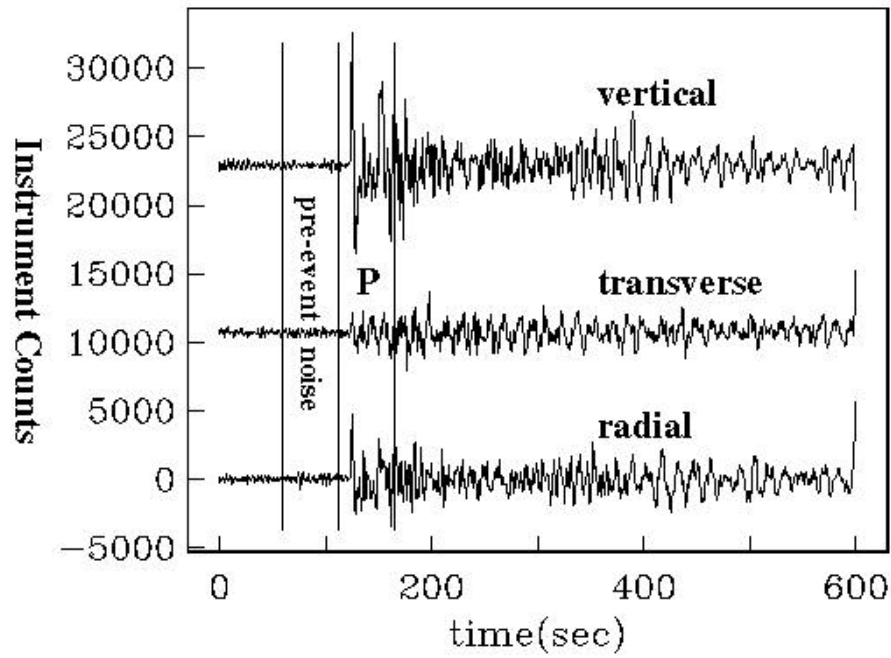
We recommend continued use of back-azimuth and range-dependent receiver functions to characterize scattering at broadband seismic monitoring stations within the verification system of the Comprehensive Nuclear-Test-Ban Treaty (CTBT). Data analysis from our preliminary suite of stations suggests that a 1-D anisotropic crustal structure is appropriate for modeling a significant portion of crustal scattering in teleseismic signals. Even where significant 3-D structure is evident (PET), 3-D effects are superimposed on strong scattering from what appears to be finely-spaced horizontal, or gently dipping, layers.

REFERENCES

- Abers, G. A., X. Hu, and L. R. Sykes, Source scaling of earthquakes in the Shumagin region, Alaska: Time-domain inversions of regional waveforms, **Geophys. J. Inter.**, **123**, 41--58, 1995.
- Ammon, C. J., The isolation of receiver effects from teleseismic P waveforms, **Bull. Seism. Soc. Amer.**, **81**, 2504-2510, 1991.
- Babuska, V., and Cara, M., **Seismic Anisotropy in the Earth**, Kluwer Academic, Dordrecht, 1991.
- Bostock, M. G., Anisotropic upper-mantle stratigraphy and architecture of the Slave craton, **Nature**, **390**, 393-395, 1997.
- Cassidy, J. F., Numerical experiments in broadband receiver function analysis, **Bull. Seism. Soc. Amer.**, **82**, 1453--1474, 1992.
- Gorbatov, A., V. Kostoglodov, G. Suarez, and E. Gordeev, Seismicity and structure of the Kamchatka subduction zone, **J. Geophys. Res.**, **102**, 17883-17898, 1997.

- Helbig, K., **Foundations of Anisotropy for Exploration Seismics**, Pergammon/Elsevier Science, Oxford, 1994.
- Hudson, J. A., Wave speeds and attenuation of elastic waves in material containing cracks, **Geophys. J. Roy. Astron. Soc.**, **64**, 133--150, 1981.
- Kosarev, G. L., Makeyeva, L. I. and Vinnik, L. P., Anisotropy of the mantle inferred from observations of P to S converted waves, **Geophys. J. Roy. Astron. Soc.**, **76**, 209--220, 1984.
- Langston, C. A., The effect of planar dipping structure on source and receiver responses for constant ray parameter, **Bull. Seism. Soc. Amer.**, **67**, 1029--1050, 1977.
- Levander, A. R., and Hollinger, K., Small-scale heterogeneity and large-scale velocity structure of the continental crust, **J. Geophys. Res.**, **97**, 8797--8804, 1992.
- Dueker, K. D., and A. F. Sheehan, Mantle discontinuity structure from midpoint stacks of converted P to S waves across the Yellowstone hotspot track, **J. Geophys. Res.**, **102**, 8313-8327, 1997.
- Levin, V., and J. Park, Crustal anisotropy beneath the Ural mtns foredeep from teleseismic receiver functions, **Geophys. Res. Letts**, **24**, 1283-1286, 1997.
- Levin, V., and J. Park, P-SH conversions in a flat-layered medium with anisotropy of arbitrary orientation, **Geophys. J. Int.**, **131**, 253-266, 1997.
- Levin, V., and J. Park, A P-SH conversion in layered media with hexagonally symmetric anisotropy: A cookbook, **Pure and Applied Geophysics**, **151**, 669-697, 1998.
- Owens, T. J., and Crosson, R. S., Shallow structure effects on broad-band teleseismic P waveforms, **Bull. Seism. Soc. Amer.**, **77**, 96-108, 1988.
- Park, J., Lindberg, C. R., and F. L. Vernon III, Multitaper spectral analysis of high-frequency seismograms. **J. Geophys. Res.**, **92**, 12675--12684, 1987.
- Park, J., Surface waves in layered anisotropic structures, **Geophys. J. Int.**, **126**, 173-184, 1996.
- Savage, M., Lower crustal anisotropy or dipping boundaries? Effects on receiver functions and a case study in New Zealand, **J. Geophys. Res.**, **103**, 15069-15087, 1998.
- Thomson, D. J., Spectrum estimation and harmonic analysis, **IEEE Proc.**, **70**, 1055-1096, 1982.
- Vernon, F. L., J. Fletcher, L. Carroll, A. Chave and E. Sembrera, Coherence of seismic body waves from local events as measured by a small-aperture array, **J. Geophys. Res.**, **96**, 11981--11996, 1991.
- Wu, R.-S., Wide-angle elastic wave one-way propagation in heterogeneous media and an elastic wave complex screen method, **J. Geophys. Res.**, **99**, 751--766, 1994.

Station PET: 9/6/93 New Ireland Event, Mb=6.2



Station PET: 10/5/93 Banda Sea Event, Mb=5.9

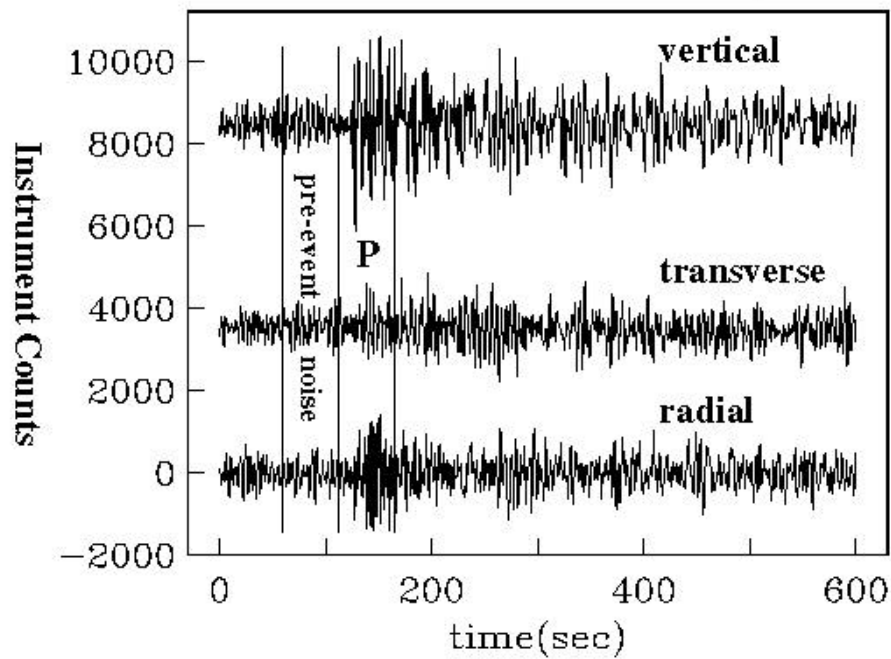
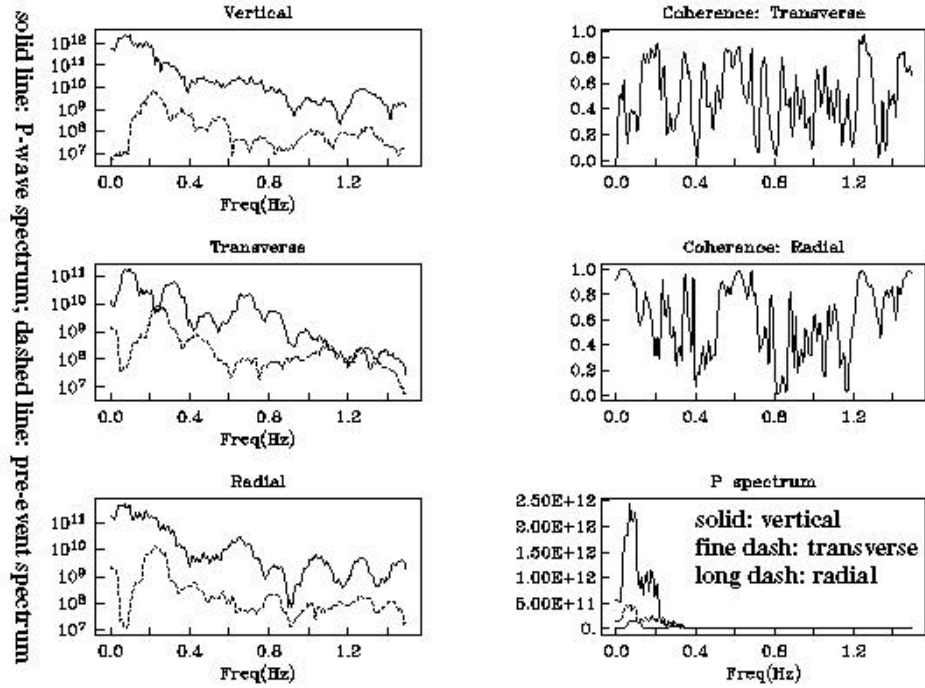


Figure 1. P-waves recorded at PET (Petropavlovsk-Kamchatsky, Russia). Data windows for spectral receiver-function analysis are indicated.

Station PET: 9/6/93 New Ireland Event, Mb=6.2



Station PET: 10/5/93 Banda Sea Event, Mb=5.9

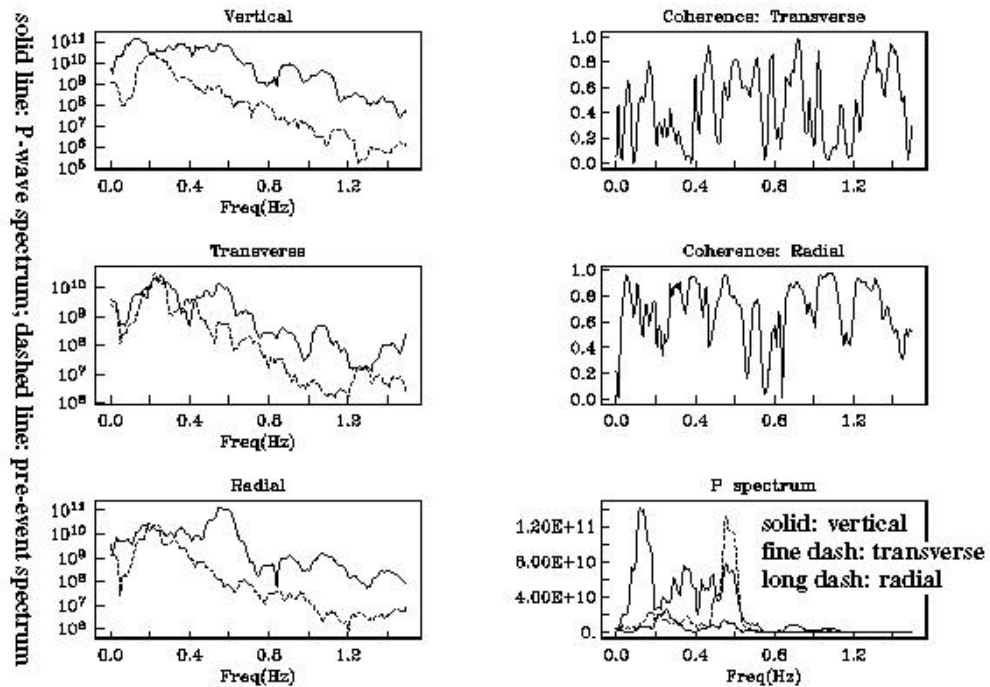
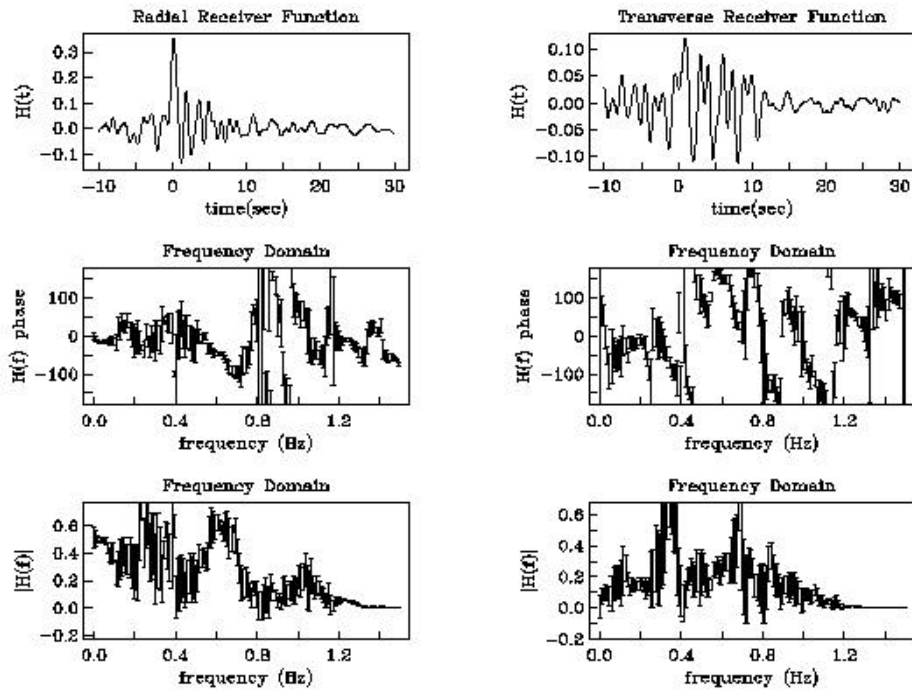


Figure 2. Multitaper spectral-correlation receiver function analysis: computations. Left-column plots compare the signal and pre-event noise of different components. Right-column plots show the coherences of radial and transverse seismic motion with the vertical motion. Note that both P waves have weak signal above 0.7 Hz.

Station PET: 9/6/93 New Ireland Event, Mb=6.2



Station PET: 10/5/93 Banda Sea Event, Mb=5.9

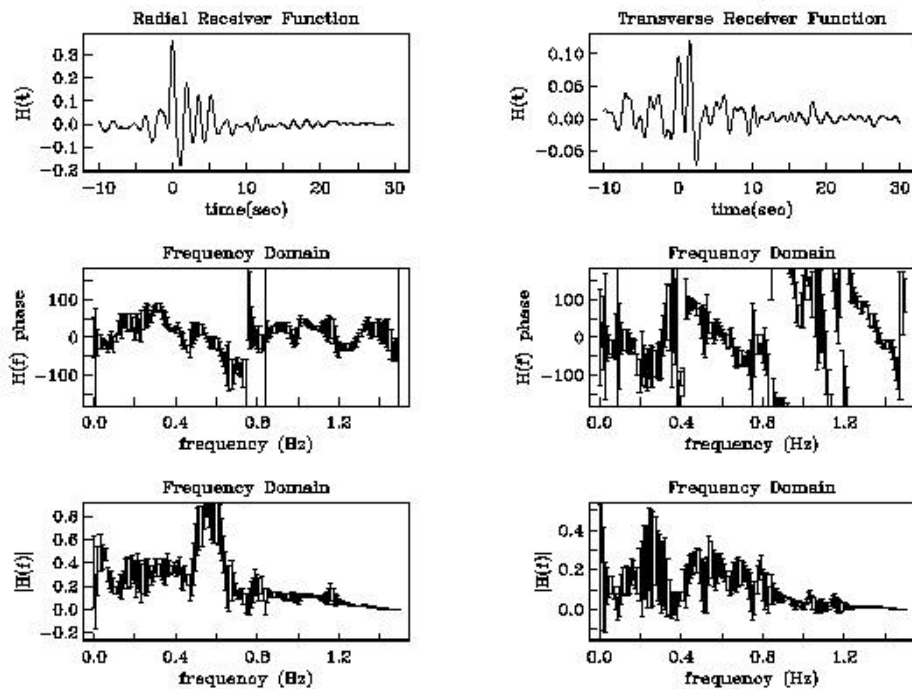


Figure 3. Multitaper spectral-correlation receiver function analysis: results. Left-column plots show radial-component Rf's in both time and frequency domains. Right-column plots show transverse-component Rf's. Oscillations in the time-domain Rf's at negative times are diagnostic of the Rf uncertainty.

ARU: radial RF sweep, 1989-98 data

Freq cutoff 1.5 Hz

Freq cutoff 3.0 Hz

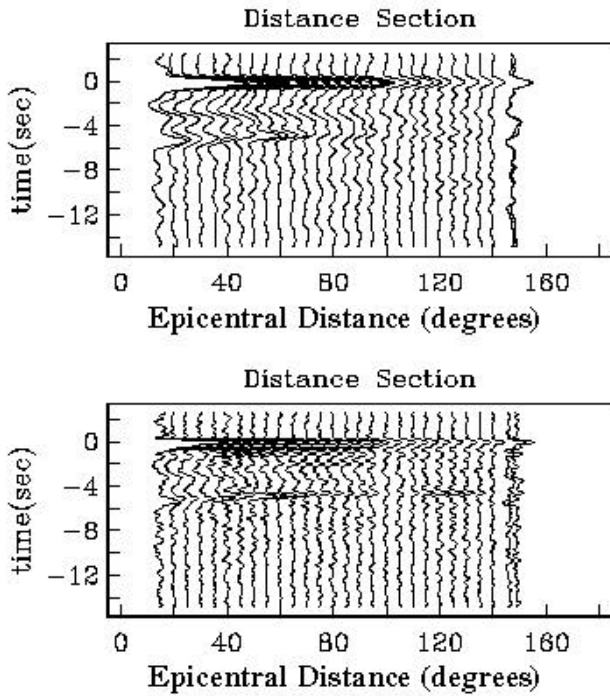


Figure 4: Range dependence of receiver functions for station ARU (Arb Settlement, Russia). RF sections for 1.5-Hz and 3.0-Hz cutoff frequencies are plotted. The composite section uses 442 seismic events. Note that several crustal-scattered waves, including the prominent Moho Ps phase at 5-sec delay, can be traced through nearly all of the 3.0-Hz section, suggesting strong horizontal layering.

ARU: RF sweeps, 1989-98 data
Frequency cutoff 1.5 Hz

Radial

Transverse

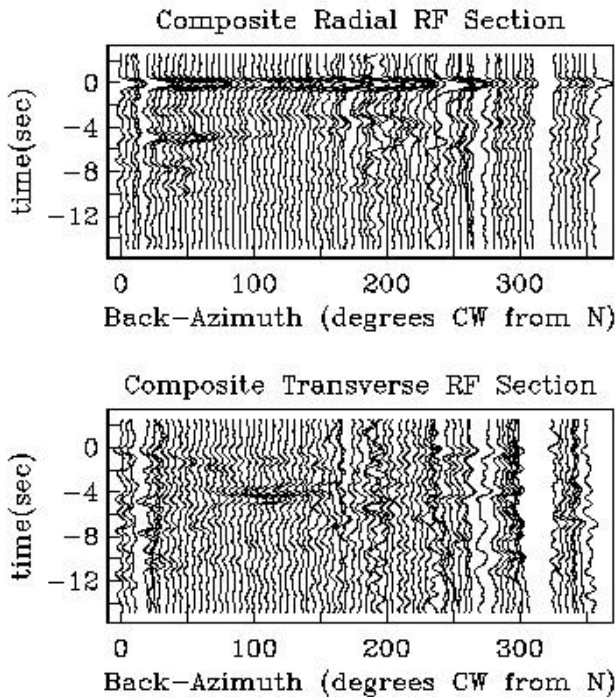


Figure 5: Back-azimuth dependence of receiver functions for station ARU (Arb Settlement, Russia). Note the strong transverse pulses at 4-5-sec delay. These pulses centered on 120° and 280° back-azimuth have reversed polarity. This can be modelled with a strongly anisotropic layer (>10%) in the lower crust. Transverse RF amplitude is boosted by factor of two for visual comparison.

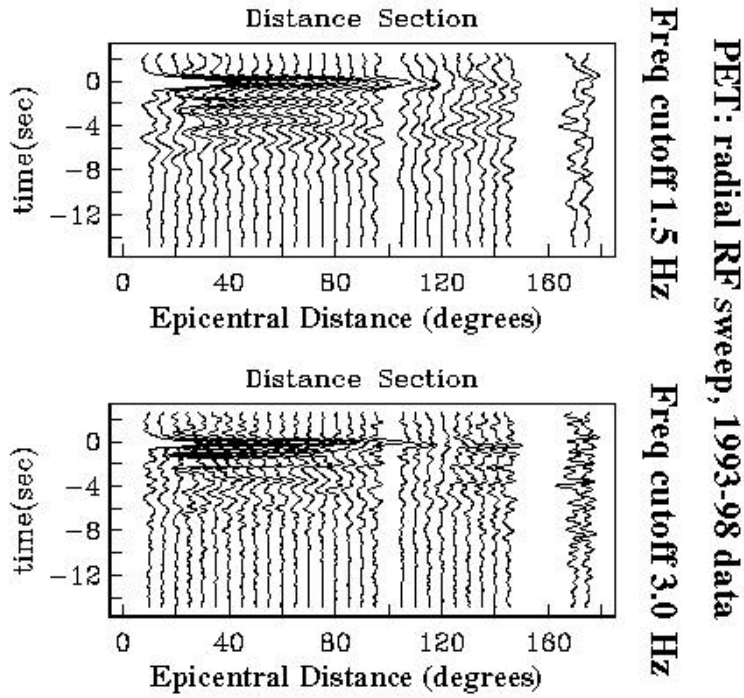


Figure 6: Range dependence of receiver functions for station PET (Петропавловск-Камчатский, Russia). RF sections for 1.5-Hz and 3.0-Hz frequency cutoffs are plotted. The composite section uses 241 seismic events.

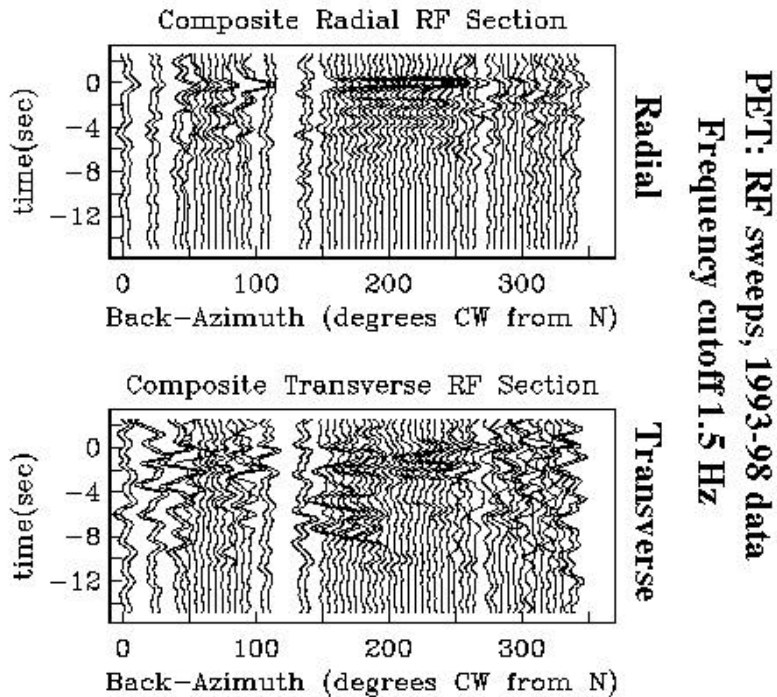


Figure 7: Back-azimuth dependence of receiver functions for station PET (Петропавловск-Камчатский, Russia). Note the strong transverse pulses at 7- to 10-sec time delay at 150°-200° back-azimuth. This signal appears to be a complex P-to-S conversion from the steeply-dipping slab beneath PET. Transverse RF amplitude is boosted by factor of two for visual comparison.